Journal of Water Resource and Protection, 2025, 17(12), 976-1003
https://www.scirp.org/journal/jwarp
ISSN Online: 1945-3108
ISSN Print: 1945-3094

Spatiotemporal Variations of Chemical Compositions through Empirical Modeling in Bartlett Pond, Laredo, Texas

Maya Prakash Bhatt[1*], Ganesh Bahadur Malla[2], Diana Elisa Nuño[1], Seema Bhatt[1], Alfred Addo-Mensah[1]

[1]Department of Biology and Chemistry, Texas A&M International University, Laredo, USA
[2]Department of MCGP, University of Cincinnati-Clermont, Batavia, USA
Email: *maya.bhatt@tamiu.edu

How to cite this paper: Bhatt, M.P., Malla, G.B., Nuño, D.E., Bhatt, S. and Addo-Mensah, A. (2025) Spatiotemporal Variations of Chemical Compositions through Empirical Modeling in Bartlett Pond, Laredo, Texas. *Journal of Water Resource and Protection*, **17**, 976-1003.
https://doi.org/10.4236/jwarp.2025.1712051

Received: November 17, 2025
Accepted: December 27, 2025
Published: December 30, 2025

Abstract

Surface water samples were collected from a small, shallow wetland Bartlett pond in Laredo, Southern Texas, to investigate the factors controlling water quality parameters and their spatiotemporal variation within the ecosystem. The major cations and anions occurred in the following order: $Na^+ \gg Ca^{2+} > Mg^{2+} \approx K^+$ and $HCO_3^- \approx Cl^- > SO_4^{2-} \gg NO_3^- \gg PO_4^{3-}$, respectively. Marine aerosols were the primary source for most of the magnesium (76%) and sodium (73%) concentrations, while contributing only minor proportions of potassium (17%) and calcium (4.5%). In addition to contributions from marine aerosols, the weathering of minerals, primarily carbonate and siliciclastic, plays a key role in regulating the pond's water chemistry. We observed strong seasonal control on chemical compositions but minor spatial variation trends within the pond. A comprehensive multivariate regression analysis was conducted to evaluate the biogeochemical controls on water quality in Bartlett Pond across seasonal cycles. Seventeen major physicochemical parameters including water temperature, pH, EC, TDS, major base cations (Ca^{2+}, Mg^{2+}, Na^+, K^+), anions (Cl^-, NO_3^-, SO_4^{2-}, PO_4^{3-}, HCO_3^-), and other parameters such as Hardness, Alkalinity, SAR, and Boron were analyzed through 43 predictive models, yielding a total of 265 regression coefficients. The models explained substantial proportions of variance (R^2 = 0.64 to 1.00), revealing strong interdependencies among ionic constituents. Obviously, Total Dissolved Solids (TDS) and Electrical Conductivity (EC) exhibited robust predictive capacity for ionic strength, while NO_3^-, PO_4^{3-}, and SAR emerged as sensitive indicators of both geochemical weathering and anthropogenic inputs. Phosphate appeared as a limiting nutrient, and nitrate drastically de-

creased during summer months, suggesting increased photosynthetic activities and consequently gross primary productivity (GPP) increases within this shallow pond. Seasonal variations reflected shifts between carbonate equilibrium, nutrient cycling, and evaporative concentration effects. The integrated regression framework provides quantitative insight into the hydrological-geochemical coupling governing small pond systems under variable seasonal influences.

Keywords

Major Solutes, Sea-Salt Correction, Weathered Contribution, Multivariate Hydrochemical Modeling, Bartlett Pond

1. Introduction

Water is a vital natural resource which is essential for the survival of all living organisms, including flora and fauna, and for regulating biogeochemical cycles and sustaining the ecological balance of landscapes [1]-[5]. Freshwater is a limited resource that is increasingly impacted by various anthropogenic factors, such as urbanization, industrialization, climate change, extreme weather events, increased frequency of droughts, and permanent water loss globally [6]-[9]. Wetlands and other aquatic habitats are seriously threatened by human activities, leading to a decline in both habitat quality and overall biodiversity [10]-[14]. According to recent analyses, more than 4.4 billion people, representing over half of the global population, do not have access to safe drinking water, a figure that is more than double the estimate reported in 2020 [4] [15]-[18].

Wetlands provide critical ecosystem services that preserve and purify surface water and are crucial for harboring biodiversity [19] [20]. Wetland ecosystems cover about six percent of the Earth's total land surface and are necessary for biogeochemical cycles, offering ecosystem services such as flood control, groundwater recharge, drought mitigation, habitat for diverse plant and animal species, and water quality protection [2] [12] [21]-[29]. Wetlands provide society with up to US$ 39 trillion in annual economic benefits, yet they are disappearing at a rate of 0.52% annually [29]. Maintaining healthy, functioning wetlands is far more cost-effective than restoring degraded ones, and the Global Wetlands Outlook 2025 (GWO) calls for immediate action from policymakers, businesses, and society [29]. Globally, wetlands are decreasing due to anthropogenic disturbances, as many are being altered, drained, or otherwise degraded [30]. Wetlands are often called the "kidneys of the earth" because they filter pollutants, sediments, and nutrients over long periods, thereby maintaining healthy ecosystem functioning [12] [22] [31] [32].

Ponds represent more than 90% of the estimated 304 million standing water bodies on Earth, accounting for more than 30% of the total global standing water by surface area [33] [34]. In the United States, wetlands have faced dramatic loss, with southern states such as Florida and Texas experiencing rapid urbanization

that has intensified wetland degradation [35]. Texas has experienced disproportionately high wetland-loss rates, especially in metropolitan areas such as Houston and Dallas, giving the state the second-highest annual wetland-loss rate in the country [35]. Cunningham and Cunningham (2021) [26] documented that about half of U.S. wetlands have disappeared, primarily due to agricultural drainage and other human activities. Laredo, Texas, is a metro area that includes three main tributaries, such as Chacon Creek, Manadas Creek, and Zacate Creek of the Rio Grande, and water discharge appears to be decreasing in recent years due to rising temperatures. There are several ponds within Laredo, Texas, including a large lake, Casa Blanca. Texas has more than 1.26 million acres of freshwater in lakes, ponds, and reservoirs based on an estimate from 2013, and an additional 2.1 million acres of water are in the bays and estuaries along the Texas coast [36]. There are over 200 major reservoirs and over 5000 smaller reservoirs and bodies of water like lakes and ponds in Texas [36].

Laredo is known for its high biodiversity, particularly its local and migratory bird populations, which contribute to the ecological richness of Bartlett Pond and surrounding habitat [12]. Texas has various aviary populations, with over 650 species residing in Texas and many migrating to the area surrounding Bartlett Pond [12] [37]. With Laredo's increasing population, an increase in human disturbance could affect bird distribution and their habitats, as surface water bodies are receiving higher amounts of pollutants, including increased sediment loads and trace metals [12] [13] [38]. High concentrations of trace elements have been found in water and sediments and have accumulated in fish found in Bartlett Pond [12] [13]. These trace elements do not undergo biodegradation and create hazardous impacts on the ecosystem and enter through the food chain, posing significant ecological and environmental risks [12] [39]-[41].

It is extremely important to separate the chemical concentration of base cations and sulfate from sea-salt contributions to understand the release rates of these chemical species from chemical weathering processes [42]. We used the molar ratios of elements in seawater to estimate the sea-salt-derived ions based on earlier reported studies from different regions [43]-[45].

The objective of this study was to assess the controlling factors of the major chemical species within Bartlett Pond and evaluate the role of the spatiotemporal dynamics of chemical species. We used comprehensive multivariate regression analysis to evaluate the biogeochemical controls on water quality in Bartlett Pond across seasonal cycles. We recommend that local authorities and environmental conservation organizations incorporate these findings into future wetland-management strategies for Laredo, Texas, and contribute to broader regional and global wetland-conservation efforts.

2. Study Area

The Bartlett Pond, an urban retention wetland located in the Bartlett Soccer Complex of El Jovita Idar's El Progresso Park in Laredo, Texas, is used for recreational

purposes, including catch-and-release fishing, and was historically used as a drainage basin for Zacate Creek [12] [13]. The wetland ecosystem consists of the Bartlett Pond (27.554722˚N 99.473889˚W), an urban retention pond with a maximum depth of 4.26 meters and captures surface water from surrounding neighborhoods [12] (**Figure 1**). Two inlets (BPS 1 and BPS 4) in the pond allow surface runoff to enter the pond through subsurface pipelines. Significant accumulation of trace metals has been reported in the pond's water, and high concentrations have been detected in fish species such as bass and tilapia, as well as in sediment samples [12] [13]. The accumulation of trace metals degrades water quality and threatens the ecological health of the pond ecosystem. Trace metal contaminants were tested in water and sediment samples, and their bioaccumulation in bass and tilapia was assessed in our previous studies [12] [13]; however, a seasonal water quality assessment has not been previously conducted. A detailed description of the study site is provided in Bhatt *et al.* (2024b) [12].

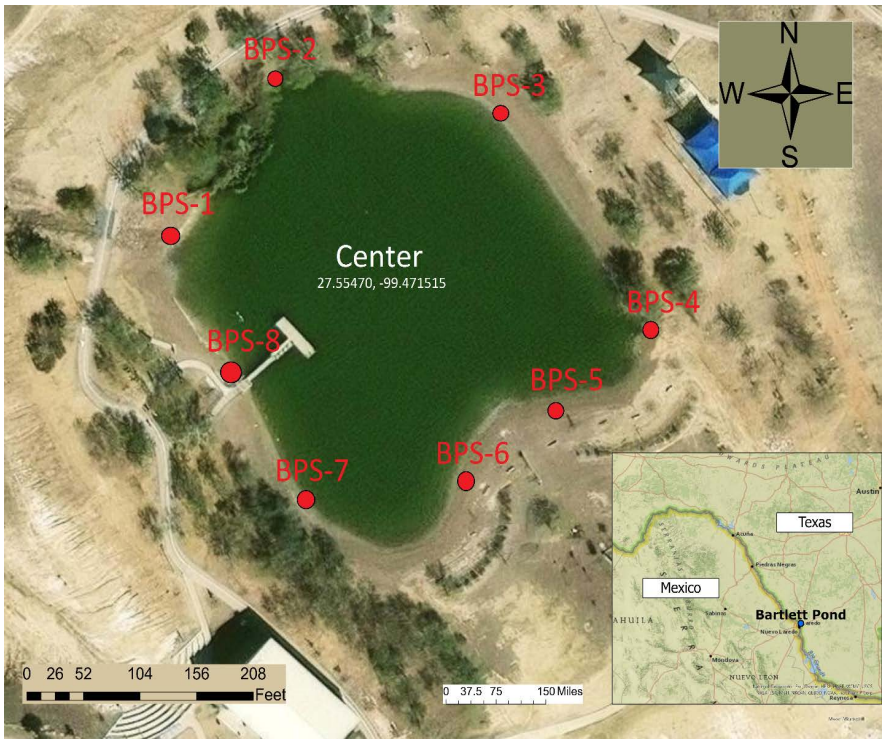

Figure 1. Sampling locations in Bartlett Pond, Laredo, Southern Texas. Trace metal concentrations in water and sediments of this pond have been reported in our earlier studies [12] [13].

Laredo is situated at an altitude of 127.41 m a.s.l. on the Mexican border in Southern Texas, covering an area of approximately 265.7 km^2, much of which is surrounded by forest. Annual rainfall averages 525.3 mm, and the mean annual temperature is 23.8˚C. The average temperature ranges from 8.9˚C in December to 31.7˚C in August. August is the hottest month of the year, with temperatures ranging from a minimum of 25.0˚C to a maximum of 38.3˚C [46].

3. Materials and Methods

3.1. Sample Collection

Bartlett pond water samples were collected from eight different locations, with a total of 24 samples across three seasons: October 2024, February 2025, and July 2025 (**Figure 1**). Surface runoff from urban areas enters the pond through two main inlets: BPS 1, which receives the highest volume of runoff, and BPS 4, which conveys runoff via a pipe from the highway and airport areas [12]. Physical parameters such as water temperature, pH, EC, and DO were measured in situ during sampling and rechecked in the laboratory. Samples were collected in 250 mL acid-washed polyethylene bottles, refrigerated at the Texas A&M International University (TAMIU) laboratory, and shipped on ice to the Soil and Water Testing Laboratory at Texas A&M University (TAMU) in College Station for the analysis of major base cations (Na^+, K^+, Mg^{2+}, Ca^{2+}), major anions (Cl^-, NO_3^-, SO_4^{2-}, HCO_3^-, PO_4^{3-}), hardness, alkalinity, sodium adsorption ratio (SAR), and boron. Carbonate ions were not detected at any sampling location.

3.2. Analytical Methods

Water temperature, pH, EC, and DO were measured at the time of sampling by using a Thermo Scientific™ Orion Star™ A329 handheld meter. Chloride was determined by ion chromatography following method 300.0 [47]. NO_3-N was measured by reduction of nitrite (NO_2-N) to nitrate by using a cadmium column followed by spectrophotometric measurement [48]. Sulfate concentrations were calculated from total sulfur [48]. Ammonium (NH_4-N) was measured by spectrophotometric measurement [48]. Fluoride was measured directly using a fluoride selective electrode [48].

Samples were filtered through 0.45 μm polycarbonate filters for Na, K, Mg, Ca, S, P, Fe, Zn, Cu, Mn, As, Ba, Cd, Cr, Ni, and Pb analysis by using Inductively Coupled Plasma Atomic Emission Spectroscopy (ICP-AES) [48]. Carbonate and bicarbonate were determined by titration using sulfuric acid [48]. Alkalinity was calculated from carbonate and bicarbonate concentrations, and hardness was calculated from Ca and Mg concentrations [48]. TDS was calculated by summing the cations and anions. Sodium absorption ratios (SAR) were calculated from sodium, calcium, and magnesium concentrations. Charge balance error was determined by dividing the sum of cations by the sum of anions and was less than 5% for all samples [48].

4. Results

4.1. Seasonal Variation in Water Temperature at Bartlett Pond

Physical and chemical parameters of Bartlett Pond, located in Laredo, southern Texas, were monitored from October 2024 to July 2025 to capture seasonal variations across fall, spring, and summer. A total of 24 samples (eight per season) were collected for comparative analysis. The mean water temperature and standard de-

viation for each season are summarized in Table 1. The observed seasonal averages were 24.6˚C ± 0.2˚C in fall, 16.5˚C ± 0.2˚C in spring, and 31.9˚C ± 1.5˚C in summer, reflecting marked thermal variability consistent with regional climatic patterns. Such a wide variation in temperature within Bartlett Pond controls chemistry, primarily carbon and nutrients, as discussed with evidence provided within the relevant section below.

Table 1. Seasonal variation in water temperature at Bartlett Pond.

Season	Sample Size (n)	Average (˚C)	Standard Deviation (˚C)
Fall	8	24.6	0.2
Spring	8	16.5	0.2
Summer	8	31.9	1.5

4.2. Seasonal Variation and Statistical Significance of Water Quality Parameters

To examine seasonal variation in the physical and chemical parameters of Bartlett Pond, an Analysis of Variance (ANOVA) test was performed to evaluate the null hypothesis that seasonal temperature differences exert no significant influence on the measured parameters. The first column of Table 2 lists all elements under study with their respective units, while columns 2 - 4 present the seasonal mean ± standard deviation for fall, spring, and summer, respectively. Columns 5 - 7 provide the corresponding Fisher's F-statistic, degrees of freedom (DF), and *p*-values. Statistically significant results, where the null hypothesis was rejected, are indicated by a palm branch (🌿) in the final column.

Table 2. Seasonal ANOVA results for physical and chemical parameters of Bartlett Pond.

Element	Fall Mean ± SD	Spring Mean ± SD	Summer Mean ± SD	F	DF	P-value
pH	8.80 ± 0.13	8.88 ± 0.23	8.54 ± 0.97	0.729	(2, 21)	0.494
DO (mg/L)	5.60 ± 2.82	9.60 ± 1.02	7.69 ± 5.55	2.413	(2, 21)	0.114
EC (µS/cm)	753.9 ± 18.0	895.0 ± 3.1	852.5 ± 76.3	20.433	(2, 21)	**<0.001** 🌿
TDS (mg/L)	501.3 ± 9.8	578.4 ± 23.1	562.4 ± 49.3	13.023	(2, 21)	**<0.001** 🌿
Ca^{2+} (mg/L)	64.0 ± 1.7	64.8 ± 0.9	49.0 ± 8.7	23.702	(2, 21)	**<0.001** 🌿
Mg^{2+} (mg/L)	8.10 ± 0.4	11.63 ± 0.5	12.25 ± 0.7	132.860	(2, 21)	**<0.001** 🌿
Na^{+} (mg/L)	72.8 ± 1.5	95.4 ± 0.9	107.3 ± 7.9	111.979	(2, 21)	**<0.001** 🌿
K^{+} (mg/L)	9.3 ± 0.5	10.0 ± 0.0	12.1 ± 0.8	58.608	(2, 21)	**<0.001** 🌿
Cl^{-} (mg/L)	100.1 ± 6.2	126.6 ± 0.7	130.6 ± 12.5	33.579	(2, 21)	**<0.001** 🌿
NO_3^{-} (mg/L)	1.93 ± 1.15	2.35 ± 0.09	0.04 ± 0.09	27.244	(2, 21)	**<0.001** 🌿
SO_4^{2-} (mg/L)	98.8 ± 4.7	118.0 ± 1.3	131.6 ± 13.1	33.374	(2, 21)	**<0.001** 🌿

Continued

PO_4^{3-} (mg/L)	0.03 ± 0.06	0.02 ± 0.02	0.12 ± 0.12	5.984	(2, 20)	**0.009**#
HCO_3^- (mg/L)	146.3 ± 6.3	149.5 ± 23.7	119.0 ± 40.6	2.989	(2, 21)	0.072
Hardness (mg/L)	192.5 ± 5.0	209.1 ± 2.9	172.0 ± 21.9	16,215	(2, 21)	**<0.001**#
Alk (mg/L)	120.1 ± 5.2	122.8 ± 19.4	97.5 ± 33.3	3.056	(2, 21)	0.068
SAR	2.29 ± 0.04	2.88 ± 0.05	3.58 ± 0.36	74.373	(2, 21)	**<0.001**#
B (mg/L)	0.27 ± 0.01	0.31 ± 0.00	0.29 ± 0.03	19.874	(2, 21)	**<0.001**#

Note: # = Statistically significant.

The Analysis of Variance (ANOVA) test revealed significant seasonal differences in several physical and chemical parameters of Bartlett Pond, indicating pronounced temporal variability in water quality between fall, spring, and summer. Parameters such as electrical conductivity (EC), total dissolved solids (TDS), calcium (Ca^{2+}), magnesium (Mg^{2+}), sodium (Na^+), potassium (K^+), chloride (Cl^-), nitrate (NO_3^-), sulfate (SO_4^{2-}), phosphate (PO_4^{3-}), hardness, sodium adsorption ratio (SAR), and boron (B) showed statistically significant variations ($p < 0.05$), while pH, dissolved oxygen (DO), bicarbonate (HCO_3^-), and alkalinity did not exhibit significant differences among seasons. These variations likely reflect seasonal influences of temperature, evaporation, biological activity, and hydrological inputs on pond chemistry in a semi-arid environment.

4.3. Significant Temporal Variations

The electrical conductivity (EC) varied significantly ($p < 0.001$), increasing from fall (753.9 µS/cm) to spring (895.0 µS/cm) before a slight decline in summer (852.5 µS/cm). The pattern indicates enhanced ionic concentration from evaporation and limited dilution during warmer months, reflecting changing hydrological balance across seasons. Total dissolved solids (TDS) followed a similar trend to EC, with higher values in spring and summer ($p < 0.001$). Elevated TDS levels suggest intensified mineral dissolution and accumulation of solutes under reduced precipitation and increased evaporation. Calcium (Ca^{2+}) concentrations declined significantly in summer ($p < 0.001$), dropping from ~64 mg/L in fall and spring to 49 mg/L. This reduction is likely to result from calcium carbonate precipitation driven by higher temperatures and pH changes. Magnesium (Mg^{2+}) increased steadily from fall to summer ($p < 0.001$), indicating concentration through evaporation and possibly enhanced mineral weathering or exchange with sediments during drier periods. Sodium (Na^+) exhibited a pronounced rise ($p < 0.001$) from 72.8 mg/L in fall to 107.3 mg/L in summer. The progressive accumulation of sodium ions suggests evaporative concentration and reduced freshwater inflow during the hot season. Potassium (K^+) also increased significantly across seasons ($p < 0.001$), with concentrations highest in summer (12.1 mg/L). This may reflect both evaporative effects and the release of ions from organic matter decomposition.

The chloride (Cl^-) concentrations rose sharply ($p < 0.001$) from fall (100.1 mg/L) to summer (130.6 mg/L). As a conservative ion, chloride serves as a strong indicator of evaporative concentration and ionic accumulation. Nitrate (NO_3^-) showed a dramatic decline ($p < 0.001$), from 1.93 mg/L in fall to only 0.04 mg/L in summer. The decrease is likely due to biological uptake and denitrification under elevated temperatures and reduced oxygen levels. Sulfate (SO_4^{2-}) concentrations increased significantly ($p < 0.001$), with the highest levels in summer (131.6 mg/L), suggesting continued mineral weathering and solute concentration from evaporation and runoff inputs. Phosphate (PO_4^{3-}) showed moderate but significant variation ($p = 0.009$), with summer concentrations (0.12 mg/L) exceeding those in fall and spring. This increase likely reflects enhanced organic matter decomposition and sediment water nutrient exchange. These major ionic concentrations from Bartlett pond in Laredo, Texas, appeared several fold higher than those from the high-altitude streams, lakes, and ponds from Langtang and the Mt. Everest region of the Himalayas, suggesting the role of climate, geology, and proximity to the coast as the main factors for such differences [49]-[51]. Water hardness varied significantly ($p < 0.001$), peaking in spring (209.1 mg/L) and decreasing in summer (172.0 mg/L). This pattern mirrors the combined effects of Ca^{2+} and Mg^{2+} dynamics and carbonate precipitation during warm periods. Sodium Adsorption Ratio (SAR*)* values increased consistently from fall (2.29) to summer (3.58; $p < 0.001$), driven by elevated Na^+ relative to Ca^{2+} and Mg^{2+}. This trend may indicate rising sodality risk, particularly under prolonged dry conditions. The metalloid, boron (B), concentrations exhibited small but significant variation ($p < 0.001$), peaking in spring (0.31 mg/L) and slightly decreasing in summer. The pattern aligns with evaporative concentration and geochemical cycling of trace elements in semi-arid systems.

4.4. Spatial-Temporal Multivariate Modeling of Water Quality Parameters

Bhatt *et al.* (2024b) [12] conducted a comprehensive multivariate modeling study of trace elemental concentrations in Bartlett Pond; however, their analysis did not account for seasonal variability and major ionic compositions. Building on the findings presented in the preceding section, which revealed significant seasonal differences in most major water quality parameters, it became necessary to develop separate predictive models for each season. Accordingly, distinct multivariate models were constructed for fall, spring, and summer datasets to better capture the spatial-temporal dynamics of pond chemistry.

The Backward Regression Method was employed for this analysis to systematically refine each model by removing statistically insignificant predictors, thereby enhancing model parsimony and interpretability. This approach minimizes multicollinearity among variables and ensures that only the most influential parameters are retained, providing a robust representation of the seasonal relationships governing the chemical composition of Bartlett Pond.

Table 3. Spatial-multivariate models of water quality parameters in Bartlett Pond.

Model #	Measured Parameters	Season	Predictive Model	R^2 value
1	pH	All	$\widehat{pH} = 5.05 + 0.01EC - 0.12Mg^{2+} - 0.06Cl^{-} + 0.16NO_3^{-} + 0.06SO_4^{2-}$	0.901
2	Dissolved Oxygen	All	$\widehat{DO} = 93.90 + 0.163EC - 1.96Ca^{2+} - 3.67K^{+} + 0.26SO_4^{2-} + 30.93PO_4^{3-} - 34.01SAR$	0.645
3.1	Electrical Conductivity	Fall	$\widehat{EC} = 512.39 - 11.11pH1.91Na^{+}4.44NO_3^{-} + 36.94PO_4^{3-} - 0.82Alk - 125.56SAR + 2175.56B$	1.00
3.2		Spring	$\widehat{EC} = 758.36 + 1.26pH - 0.04TDS - 8.07Mg^{2+} + 0.71Cl^{-} + 32.70NO_3^{-} - 108.32PO_4^{3-} + 27.35SAR$	1.00
3.3		Summer	$\widehat{EC} = 1561.37 - 37.61pH - 4.12DO + 4.65Ca^{2+} - 34.83Mg^{2+} + 8.06NO_3^{-} - 526.04B$	1.00
4.1	Total Dissolved Solids	Fall	$\widehat{TDS} = 230.80 - 14.13pH + 1.37Na^{+} + 0.86NO_3^{-} - 9.82PO_4^{3-} + 0.26Alk - 31.44SAR + 0.44EC$	1.00
4.2		Spring	$\widehat{TDS} = 17.00 + 2.23pH + 0.97Cl^{-} + 3.07SO_4^{2-} + 34.12PO_4^{3-} + 0.93HCO_3^{-} - 24.51SAR - 0.02EC$	1.00
4.3		Summer	$\widehat{TDS} = 128.78 + 0.861K^{+} + 2.51NO_3^{-} - 0.39SO_4^{2-} - 19.48PO_4^{3-} - 10.12SAR + 0.60EC$	1.00
5.1	Ca^{2+}	Fall	$\widehat{Ca^{2+}} = 90.93 - 2.82pH + 0.11Na^{+} + 0.29NO_3^{-} + 11.31PO_4^{3-} - 0.03Alk - 28.09SAR + 211.92B$	1.00
5.2		Spring	$\widehat{Ca^{2+}} = 16.95 + 0.67pH + 0.06EC - 0.13Cl^{-} + 0.43SO_4^{2-} + 6.82PO_4^{3-} - 0.03HCO_3^{-} - 16.02SAR$	1.00
5.3		Summer	$\widehat{Ca^{2+}} = -13.20 + 0.862pH - 0.09DO - 1.26Mg^{2+} - 1.01NO_3^{-} + 0.40Hardness + 10.22B$	1.00
6.1	Mg^{2+}	Fall	$\widehat{Mg^{2+}} = 12.77 - 0.43pH + 0.08Na^{+} - 0.001NO_3^{-} + 0.37PO_4^{3-} - 0.04Alk - 1.82SAR + 9.77B$	1.00
6.2		Spring	$\widehat{Mg^{2+}} = 54.72 + 0.55pH - 0.09EC - 0.05Cl^{-} + 0.32SO_4^{2-} - 11.13PO_4^{3-} - 1.01HCO_3^{-} + 0.38SAR$	1.00
6.3		Summer	$\widehat{Mg^{2+}} = -6.00 + 0.03DO + 0.75K^{+} + 6.71NO_3^{-} + 0.03SO_4^{2-} - 2.18SAR + 46.03B$	1.00

Continued

7.1		Fall	$\widehat{Na^+} = 30.59 - 1.86pH - 6.33K^+ + 2.52NO_3^- + 10.91PO_4^{3-} - 0.18Alk - 18.50SAR + 661.29B$	1.00
7.2	Na^+	Spring	$\widehat{Na^+} = -84.22 + 1.44pH + 0.10EC - 0.14Cl^- + 0.88SO_4^{2-} + 15.44PO_4^{3-} - 0.01HCO_3^- - 1.79SAR$	1.00
7.3		Summer	$\widehat{Na^+} = 245.91 - 5.49pH - 0.60DO - 0.26Ca^{2+} - 4.87Mg^{2+} + 8.02NO_3^- - 49.17B$	1.00
8.1		Fall	$\widehat{K^+} = 4.83 - 0.29pH + 0.16Na^+ + 0.40NO_3^- + 1.72PO_4^{3-} - 0.03Alk - 2.92SAR + 104.42B$	1.00
8.2	K^+	Spring	$\widehat{K^+} = 100.91 + 3.30pH - 0.21EC + 0.27Cl^- + 0.45SO_4^{2-} + 9.60PO_4^{3-} - 0.02HCO_3^- - 5.40SAR$	1.00
8.3		Summer	$\widehat{K^+} = 32.61 - 0.78pH - 0.08DO - 0.07Cl^- + 0.65Mg^{2+} - 6.63NO_3^- - 59.47B$	1.00
9.1		Fall	$\widehat{Cl^-} = 248.15 - 13.32pH + 0.61Na^+ + 1.55NO_3^- - 1.55PO_4^{3-} - 0.80Alk - 37.55SAR + 391.19B$	1.00
9.2	Cl^-	Spring	$\widehat{Cl^-} = 43.17 + 0.15EC + 0.14K^+ + 1.07SO_4^{2-} + 7.47PO_4^{3-} - 0.03HCO_3^- - 0.56Hardness - 20.51SAR$	1.00
9.3		Summer	$\widehat{Cl^-} = 375.04 - 10.58pH - 0.95DO - 0.17Ca^{2+} - 7.00Mg^{2+} - 3.21NO_3^- - 177.24B$	1.00
10.1		Fall	$\widehat{NO_3^-} = 111.70 - 6.01pH - 0.41DO + 0.22Na^+ - 1.79PO_4^{3-} - 0.043Alk + 1.66SAR - 260.58B$	1.00
10.2	NO_3^-	Spring	$\widehat{NO_3^-} = -12.73 + 0.02EC + 0.03K^+ - 0.04Cl^- + 0.07SO_4^{2-} + 0.001HCO_3^- - 0.61SAR$	1.00
10.3		Summer	$\widehat{NO_3^-} = 0.35 - 0.02DO - 0.005Ca^{2+} + 0.12Mg^{2+} - 0.09K^+ + 0.82PO_4^{3-} - 1.47B$	1.00
11.1		Fall	$\widehat{SO_4^{2-}} = 128.40 - 5.20pH + 0.78Na^+ - 0.61NO_3^- - 7.18PO_4^{3-} - 0.51Alk - 4.23SAR + 120.36B$	1.00
11.2	SO_4^{2-}	Spring	$\widehat{SO_4^{2-}} = 101.00 - 0.15EC + 0.01TDS + 0.97Mg^{2+} + 1.07Na^+ - 0.63K^+ + 0.36Cl^- - 1.64SAR$	1.00
11.3		Summer	$\widehat{SO_4^{2-}} = 139.74 + 10.69pH - 0.72DO - 0.71Ca^{2+} - 1.96Mg^{2+} - 26.74NO_3^- - 118.35B$	1.00

Continued

12.1	PO_4^{3-}	Fall	$\widehat{PO_4^{3-}} = -8.04 + 0.25pH + 0.09Ca^{2+} - 0.01Na^{+} - 0.03NO_3^{-} + 0.002Alk + 2.48SAR - 18.73B$	1.00
12.2		Spring	$\widehat{PO_4^{3-}} = 2.98 - 0.01EC - 0.08Mg^{2+} + 0.01K^{+} - 0.01Cl^{-} + 0.02SO_4^{2-} + 0.001HCO_3^{-} + 0.10SAR$	1.00
12.3		Summer	$\widehat{PO_4^{3-}} = 3.00 - 0.08pH + 0.01DO - 0.001Ca^{2+} - 0.08Mg^{2+} + 0.53NO_3^{-} - 4.44B$	1.00
13	HCO_3^{-}	All	$\widehat{HCO_3^{-}} = 5.21 + 0.12Na^{+} + 2.08PO_4^{3-} - 0.03Hardness + 1.22Alk - 3.54SAR$	1.00
14	Alkalinity	All	$\widehat{Alk} = -8.37 + 0.04DO - 0.16Na^{+} + 0.20K^{+} - 0.02SO_4^{2-} - 3.17PO_4^{3-} + 0.82HCO_3^{-} + 0.05Hardness + 4.86SAR$	1.00
15.1	Hardness	Fall	$\widehat{Hardness} = 151.87 + 0.27pH - 0.29Na^{+} + 1.39NO_3^{-} + 26.80PO_4^{3-} + 0.03Alk - 79.77SAR + 886.17B$	1.00
15.2		Spring	$\widehat{Hardness} = 76.98 + 0.27EC + 0.24K^{+} - 1.78Cl^{-} + 1.91SO_4^{2-} + 13.32PO_4^{3-} - 0.07HCO_3^{-} - 36.57SAR$	1.00
15.3		Summer	$\widehat{Hardness} = 33.36 - 2.18pH + 0.23DO + 2.53Ca^{2+} + 3.18Mg^{2+} + 2.54NO_3^{-} - 25.83B$	1.00
16.1	Sodium Adsorption Ratio	Fall	$\widehat{SAR} = 3.24 - 0.10pH - 0.04Ca^{2+} + 0.004Na^{+} + 0.01NO_3^{-} + 0.40PO_4^{3-} - 0.001Alk + 7.55B$	1.00
16.2		Spring	$\widehat{SAR} = 6.61 + 0.02DO - 0.06Ca^{2+} + 0.01K^{+} - 0.02Cl^{-} + 0.02SO_4^{2-} - 0.04PO_4^{3-} - 0.002Alk$	1.00
16.3		Summer	$\widehat{SAR} = 9.86 - 0.12pH - 0.02DO - 0.03Ca^{2+} - 0.26Mg^{2+} + 0.44NO_3^{-} - 0.87B$	1.00
17.1	Boron	Fall	$\hat{B} = 0.43 - 0.023pH - 0.002DO + 0.001Na^{+} - 0.004NO_3^{-} - 0.006PO_4^{3-} + 0.006SAR$	1.00
17.2		Spring	$\hat{B} = 0.23 + 0.001EC + 0.007K^{+} - 0.006Cl^{-} - 0.007SO_4^{2-} - 0.612PO_4^{3-} + 0.251SAR$	1.00
17.3		Summer	$\hat{B} = 0.15 - 0.001DO + 0.022Mg^{2+} - 0.016K^{+} - 0.146NO_3^{-} - 0.001SO_4^{2-} + 0.047SAR$	1.00

Interpretation of Spatial-Temporal Multivariate Models: Table 3 presents a comprehensive suite of 17 multivariate regression models, developed to predict the spatial and temporal behavior of major physical and chemical parameters in Bartlett Pond. In total, the analysis produced 39 predictive equations, three for each season (fall, spring, and summer) where seasonal effects were significant, and single annual models for parameters showing minimal seasonal dependence. Collectively, these models comprise over 250 regression coefficients, each quantifying the partial influence of one variable on another while holding other predictors constant. Such coefficients encode detailed information on the interconnected chemical dynamics of the pond, offering a robust empirical framework for understanding system-wide geochemical interactions.

R^2 values, all near or equal to 1.00, indicate an excellent level of explanation of variance in the dependent variable, suggesting high predictive reliability within the observed dataset. Readers should interpret each equation as a statistical representation of how multiple parameters jointly influence the target element's concentration.

Model 4.1 (Fall Season): For instance, Equation 4.1 models Total Dissolved Solids (TDS) during the fall season as:

$$\widehat{\mathrm{TDS}} = 230.80 - 14.13\mathrm{pH} + 1.37\mathrm{Na}^{+} + 0.86\mathrm{NO}_3^{-} - 9.82\mathrm{PO}_4^{3-} + 0.26\mathrm{Alk} - 31.44\mathrm{SAR} + 0.44\mathrm{EC}.$$

Each coefficient represents the expected change in Total Dissolved Solids (TDS, $mg{\cdot}L^{-1}$) for a one-unit increase in that variable, holding all other parameters constant. Regression coefficient of pH = −14.13: When Pond pH increases by one unit, TDS decreases by 14.13 $mg{\cdot}L^{-1}$, assuming all other parameters remain constant. A higher pH likely promotes precipitation of dissolved minerals (e.g., $CaCO_3$), reducing the overall solute load. Regression coefficient of Na^+ = +1.37: A one $mg{\cdot}L^{-1}$ increase in sodium concentration increases TDS by 1.37 $mg{\cdot}L^{-1}$. Sodium ions contribute directly to dissolved solids, reflecting evaporative enrichment and ion exchange with surrounding sediments. Regression coefficient of NO_3^- = +0.86: A one $mg{\cdot}L^{-1}$ increase in nitrate increases TDS by 0.86 $mg{\cdot}L^{-1}$. Nitrate originates from surface runoff and organic decomposition; higher NO_3^- levels add to ionic strength and overall dissolved load. Regression coefficient of PO_4^{3-} = −9.82: A one $mg{\cdot}L^{-1}$ increase in phosphate reduces TDS by 9.82 $mg{\cdot}L^{-1}$. Elevated phosphate can promote co-precipitation with calcium and other cations (e.g., $Ca_3(PO_4)_2$ or other complexes), effectively removing solutes from the water column. Regression coefficient of Alk = +0.26: A one $mg{\cdot}L^{-1}$ increase in alkalinity increases TDS by 0.26 $mg{\cdot}L^{-1}$. Alkalinity reflects bicarbonate and carbonate ions in solution, which contribute directly to total dissolved solids. The bicarbonate variation is due to the change in temperature with seasonality, as temperature controls carbon dynamics (e.g., emissions of carbon dioxide increase from pond to atmosphere; consequently, carbon dioxide decreases within the pond), and such variation in inorganic carbon species with temperature has recently been documented by Bhatt and Malla (2025) [52]. Regression coefficient of SAR = −31.44: A one-unit increase

in the Sodium Adsorption Ratio (dimensionless) decreases TDS by 31.44 mg·L^{-1}. High SAR may enhance cation exchange and flocculation, causing some ions to precipitate or adsorb onto sediments, thereby lowering TDS in the water column. Regression coefficient of EC = +0.44: A one μS·cm^{-1} increase in electrical conductivity corresponds to a 0.44 mg·L^{-1} increase in TDS. EC measures the total ionic content of water; thus, higher conductivity directly reflects greater dissolved solid concentrations. By following this interpretive framework, readers can analyze other models in Table 3 similarly, identifying the direction and relative strength of each predictor's effect on the target variable. Together, these equations capture the multivariate structure of pond chemistry across seasons, offering valuable insights into the coupled hydrological and geochemical processes that regulate water quality in semi-arid environments such as southern Texas.

Model 4.2 (Spring Season):

$$\widehat{\mathrm{TDS}} = 17.00 + 2.23\mathrm{pH} + 0.97\mathrm{Cl}^- + 3.07\mathrm{SO}_4^{2-} + 34.12\mathrm{PO}_4^{3-} + 0.93\mathrm{HCO}_3^- - 24.51\mathrm{SAR} - 0.02\mathrm{EC}$$

Each coefficient represents the expected change in Total Dissolved Solids (TDS, mg·L^{-1}) for a one-unit increase in the respective predictor, holding all other variables constant.

Regression coefficient of pH = +2.23: A one-unit increase in pH increases TDS by 2.23 mg·L^{-1}, suggesting that moderately alkaline conditions may enhance the solubility of certain ion species (e.g., bicarbonate mobilization), resulting in slight enrichment of dissolved solids. Unlike in fall, spring conditions may not favor mineral precipitation due to lower water residence times and dynamic hydrological turnover.

Regression coefficient of Cl^- = +0.97: Each 1 mg·L^{-1} increase in chloride raises TDS by 0.97 mg·L^{-1} Chloride is a conservative ion and does not readily precipitate or undergo biogeochemical transformations, thus directly contributing to total ionic strength. This increase likely reflects evaporative concentration and external inputs from agricultural or atmospheric sources.

Regression coefficient of SO_4^{2-} = +3.07: A one mg·L^{-1} increase in sulfate increases TDS by 3.07 mg·L^{-1}. Sulfate is commonly introduced through erosion, mineral dissolution (e.g., gypsum), or nutrient inputs. In spring, enhanced runoff and soil leaching during rehydration periods can mobilize sulfate, adding significantly to the dissolved ion pool.

Regression coefficient of PO_4^{3-} = +34.12: A 1 mg·L^{-1} increase in phosphate increases TDS substantially by 34.12 mg·L^{-1}. Unlike fall, where phosphate facilitated precipitation reactions, spring conditions (with increasing biological activity, algal growth, and nutrient input) may promote solubilization, keeping phosphate and associated ionic complexes in solution. This strong effect suggests that spring phosphate availability is linked with overall mobilization of dissolved solids.

Regression coefficient of HCO_3^- = +0.93: Each 1 mg·L^{-1} increase in bicarbonate raises TDS by 0.93 mg·L^{-1}. Bicarbonate is a major component of alkalinity and contributes directly to dissolved solids. In spring, recharge from rain and

moderate temperatures may facilitate soil water CO_2 exchange and carbonate dissolution, increasing bicarbonate levels, consistent with seasonal carbon cycling dynamics (Bhatt and Malla 2025) [52].

Regression coefficient of SAR = −24.51: A one-unit increase in Sodium Adsorption Ratio reduces TDS by 24.51 mg·L^{-1}. Higher SAR may trigger cation-exchange processes and promote ion retention within soil particles or flocculation of suspended matter, resulting in the removal of dissolved ionic species from water. This highlights that sodicity influences solute stabilization and transport under spring hydrologic conditions.

Regression coefficient of EC = −0.02: A one μS·cm^{-1} increase in electrical conductivity reduces TDS marginally by 0.02 mg·L^{-1}. While EC typically reflects dissolved ion content, this weak negative relationship suggests a possible multicollinearity effect or compensatory dynamics with other strong predictors (e.g., phosphate, sulfate), which more dominantly regulate ion availability in spring waters.

Model 4.2 indicates that spring TDS is strongly influenced by nutrient-driven solubilization (particularly phosphate), geochemical dissolution processes (via sulfate and bicarbonate), and hydrologic flushing conditions. Whereas SAR exerts a stabilizing effect through ion adsorption and exchange, the influence of EC is minor compared to more chemically active constituents. Collectively, these results indicate that spring pond chemistry is governed by nutrient reactivation, runoff-induced mineral dissolution, and early-season soil-water interaction dynamics, contrasting with precipitation-dominated processes observed in the fall model.

Model 4.3 (Summer Season):

$$\widehat{\mathrm{TDS}} = 128.78 + 0.861\mathrm{K}^{+} + 2.51\mathrm{NO}_3^{-} - 0.39\mathrm{SO}_4^{2-} - 19.48\mathrm{PO}_4^{3-} - 10.12\mathrm{SAR} + 0.60\mathrm{EC}$$

Each regression coefficient reflects the expected change in Total Dissolved Solids (TDS, mg·L^{-1}) for a one-unit increase in the predictor while holding all other variables constant. The exceptionally high model fit (R^2 = 1.00) indicates that this combination of predictors fully explains the variation in TDS under summer hydrological and geochemical conditions.

Regression coefficient of K^+ = +0.861: An increase of 1 mg·L^{-1} in potassium results in a 0.861 mg·L^{-1} increase in TDS. Potassium is a mobile cation derived from mineral weathering and agricultural runoff. Under high evaporation during summer, solute concentration intensifies, allowing K^+ levels to increase and directly contribute to overall dissolved solids.

Regression coefficient of NO_3^- = +2.51: A 1 mg·L^{-1} increase in nitrate increases TDS by 2.51 mg·L^{-1}. Elevated summer temperatures accelerate organic decomposition and microbial nitrification, leading to nitrate accumulation. Additionally, agricultural irrigation and return flows may contribute to nitrate enrichment, significantly enhancing ionic load and total solute concentration.

Regression coefficient of SO_4^{2-} = −0.39: Each 1 mg·L^{-1} increase in sulfate decreases TDS by 0.39 mg·L^{-1}. This small negative relationship suggests that sulfate

may participate in mineral precipitation reactions or associate with calcium or magnesium to form insoluble compounds under concentrated summer conditions. High evaporation levels could also drive sulfate-limited buffering processes.

Regression coefficient of PO_4^{3-} = −19.48: A 1 mg·L^{-1} increase in phosphate decreases TDS by 19.48 mg·L^{-1}. This indicates that under intense summer evaporation and biological productivity, phosphate likely co-precipitates with calcium or iron (e.g., $Ca_3(PO_4)_2$) or integrates into biomass, removing dissolved ions from the aqueous phase. This is consistent with enhanced stratification and lower water turnover during hot summer months.

Regression coefficient of SAR = −10.12: A unit increase in Sodium Adsorption Ratio results in a decrease of 10.12 mg·L^{-1} in TDS. Higher SAR promotes cation exchange with sediments and may induce soil particle dispersion or enhanced adsorption of ions into clay structures. During summer, when water volumes reduce significantly, such ion retention dynamics become critically important in lowering dissolved solids.

Regression coefficient of EC = +0.60: An increase of 1 μS·cm^{-1} in electrical conductivity leads to a 0.60 mg·L^{-1} increase in TDS. This is expected as EC measures the overall ionic concentration of water, and under high summer evaporation and mineral dissolution, conductivity rises in tandem with TDS. This positive relationship confirms strong solute accumulation during the dry season.

Model 4.3 highlights the strong influence of evaporative concentration and biogeochemical activity on summer TDS variability. Potassium and nitrate emerge as key positive contributors, reflecting high solute mobility and nutrient cycling in the warm, low-flow period. In contrast, sulfate and phosphate show negative effects due to likely precipitation reactions or biological uptake under thermally enhanced conditions. SAR moderates solute concentration through ionic binding and sediment interactions, while EC acts as a robust proxy for overall mineral enrichment.

Overall, summer pond chemistries appear governed by evaporative concentration, nutrient transformation, mineral saturation effects, and ion adsorption dynamics, consistent with intensification of solute accumulation under high temperature, reduced dilution, and extended seasonal residence time.

Comparative Summary of Models 4.1 - 4.3: Across all three seasons, Total Dissolved Solids (TDS) are governed by a distinct set of physicochemical drivers, reflecting seasonal shifts in hydrology, temperature, nutrient availability, and mineral interactions. In the **fall (Model 4.1)**, TDS is primarily regulated by mineral precipitation and solute reduction pathways, with negative coefficients for pH, phosphate, and SAR indicating dominant removal mechanisms through precipitation and cation exchange. In contrast, **spring (Model 4.2)** shows strong positive contributions from phosphate, sulfate, and bicarbonate, reflecting the reactivation of nutrient cycling, increased runoff, and enhanced mineral dissolution as hydrological flows resume after winter recharge. Meanwhile, **summer (Model 4.3)** is characterized by evaporative enrichment and nutrient mobilization, with

positive contributions from potassium, nitrate, and EC, while negative effects of phosphate and sulfate indicate precipitation or biological assimilation under high temperature and concentrated conditions.

Overall, the models suggest that fall processes are dominated by solute stabilization and precipitation, spring is driven by hydrologic flushing and nutrient release, and summer promotes evaporative concentration and biogeochemical transformation. SAR consistently appears as a solute-reducing factor across all seasons, indicating the importance of cation exchange and sediment interactions in regulating ion availability. Collectively, Models 4.1 - 4.3 demonstrate that pond chemistry is governed by seasonally modulated interactions between evaporation, precipitation, nutrient cycling, and mineral equilibrium, reinforcing the significance of climate-driven hydrological variability in shaping water quality in semi-arid environments.

4.5. Seasonal Variability and Statistical Significance of Sea-Salt Contributed and Weathered Parameters in Bartlett Pond

To assess the seasonal variability of selected sea salt-contributed (denoted with SS) and non-sea salt weathered (denoted with an asterisk *) major base cations and sulfate in Bartlett Pond, a one-way Analysis of Variance (ANOVA) was conducted. The objective was to test the null hypothesis that seasonal temperature differences exert no statistically significant influence on these parameters. The results (Table 4) revealed distinct and statistically significant seasonal differences ($p < 0.05$) in all measured ions, indicating that temperature-driven processes play a critical role in regulating the geochemical behavior of sea-salt-derived constituents.

Table 4. Seasonal variability and statistical significance of sea-salt-contributed and weathered-contributed major base cations and sulfate ions in Bartlett Pond.

Base Cations and Sulfate	Fall Mean ± SD	Spring Mean ± SD	Summer Mean ± SD	F	DF	P-value
SS-Na^+ (%)	76.9 ± 3.1	74.2 ± 0.7	68.0 ± 2.0	32.425	(2, 21)	<0.001#
*Na^+ (%)	23.1 ± 3.3	25.8 ± 0.7	32.0 ± 2.0	32.425	(2, 21)	<0.001#
SS-K^+ (%)	22.5 ± 0.8	26.2 ± 0.1	22.4 ± 2.6	15.166	(2, 21)	<0.001#
*K^+ (%)	77.5 ± 0.8	73.8 ± 0.1	77.6 ± 2.6	15.166	(2, 21)	<0.001#
SS-Mg^{2+} (%)	82.7 ± 1.8	73.3 ± 3.4	72.0 ± 9.8	7.358	(2, 21)	0.004#
*Mg^{2+} (%)	17.3 ± 1.8	26.8 ± 3.4	28.0 ± 9.8	7.358	(2, 21)	0.004#
SS-Ca^{2+} (%)	3.4 ± 0.2	4.2 ± 0.1	5.8 ± 1.0	40.235	(2, 21)	<0.001#
*Ca^{2+} (%)	96.6 ± 0.2	95.8 ± 0.1	94.2 ± 1.0	40.235	(2, 21)	<0.001#
SS-SO_4^{2-} (%)	14.3 ± 0.3	15.2 ± 0.2	14.2 ± 2.6	0.959	(2, 21)	0.004#
*SO_4^{2-} (%)	85.7 ± 0.3	84.8 ± 0.2	85.8 ± 2.6	0.959	(2, 21)	0.004#

Note: SS = Sea-salt contributed; (*) Non-sea-salt (weathered) contributed; # = Statistically significant.

We present the individual results and interpretations for each ion for sea-salt-contributed and non-sea-salt (weathered) contributions as follows:

Sodium (Na^+): SS-Na^+ (%) mean values decreased markedly from 76.9 ± 3.1 in fall to 74.2 ± 0.7 in spring and 68.0 ± 2.0 in summer (F = 32.425, $p < 0.001$), indicating highly significant seasonal variation. The SS-Na^+ fraction is highest during fall, likely reflecting stronger marine aerosol input and limited dilution at lower temperatures. The decline toward summer suggests enhanced dissolution, weathering, or runoff dilution during warmer months. *Na^+ (%) displayed an inverse trend, increasing from 23.1 ± 3.3 in fall to 25.8 ± 0.7 in spring and 32.0 ± 2.0 in summer (F = 32.425, $p < 0.001$), indicating highly significant seasonal difference. The complementary rise in the weathered *Na^+ fraction implies temperature-enhanced desorption and cation exchange during the summer season, consistent with stronger weathering intensity.

Potassium (K^+): SS-K^+ (%) mean values increased from 22.5 ± 0.8 in fall to 26.2 ± 0.1 in spring, then declined slightly to 22.4 ± 2.6 in summer (F = 15.166, $p < 0.001$), indicating statistically significant ($p < 0.001$). A moderate peak in spring suggests temporary enrichment from early-season marine or atmospheric deposition before dilution and uptake in summer. *K^+ (%) varied inversely, with 77.5 ± 0.8 in fall, 73.8 ± 0.1 in spring, and 77.6 ± 2.6 in summer (F = 15.166, $p < 0.001$), showing a significant seasonal trend. The lower *K^+ during spring corresponds to greater partitioning into the weathered fraction, while its recovery in summer suggests increased mineral weathering or ion release from sediments due to enhanced weathering and/or a high rate of evaporation.

Magnesium (Mg^{2+}): SS-Mg^{2+} (%) values decreased steadily from 82.7 ± 1.8 in fall to 73.3 ± 3.4 in spring and 72.0 ± 9.8 in summer (F = 7.358, $p = 0.004$), indicating statistical significance. Fall seasonal dominance indicates lower dilution and less leaching at cooler temperatures, while summer reductions reflect increased water-mineral (rock) interaction and faster cation exchange. *Mg^{2+} (%) increased conversely from 17.3 ± 1.8 in fall to 26.8 ± 3.4 in spring and 28.0 ± 9.8 in summer (F = 7.358, $p = 0.004$), indicating significant variation with temperature. Increased weathered *Mg^{2+} during warmer months implies stronger mineral weathering and ionic mobilization from catchment sources. Figure 2 presents the total average magnesium concentration for eight Bartlett Pond water samples (BPS-1 through BPS-8), partitioned into sea-salt-corrected magnesium (SS-Mg^{2+}) and non-sea-salt weathered magnesium (*Mg^{2+}).

Across all samples, SS-Mg^{2+} constitutes the dominant fraction of total magnesium, ranging from approximately 71% to 82%, while non-sea salt weathered (*Mg^{2+}) contributes the remaining 18% to 29% (Figure 2). Samples BPS-5 and BPS-6 exhibit the highest SS-Mg^{2+} proportions (80.8% and 81.6%, respectively), suggesting the role of site-specific conditions. In contrast, BPS-1, BPS-2, and BPS-8 show relatively elevated *Mg^{2+} contributions (26% - 28%), indicating comparatively higher inputs of weathered or terrestrially sourced magnesium through urban runoff, as BPS-1 is the inlet point and BPS-2 and BPS-8 are adjacent to BPS-

1 (Figure 1). Overall, the figure highlights notable spatial variability in magnesium sourcing within Bartlett Pond, reflecting differences in both marine inputs and watershed-derived geochemical weathering.

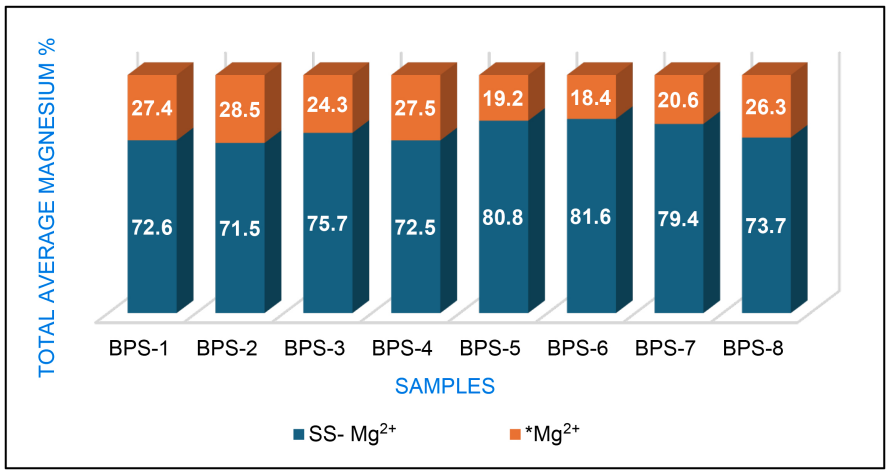

Figure 2. Relative contribution of sea salt-contributed and non-sea salt (weathered) magnesium to the total magnesium in percentage in Bartlett Pond in Laredo, Texas. SS-Mg^{2+} and *Mg^{2+} represent sea-salt and non-sea salt (weathering)-contributed magnesium, respectively.

Calcium (Ca^{2+}): SS-Ca^{2+} (%) values showed a pronounced rise from 3.4 ± 0.2 in fall to 4.2 ± 0.1 in spring and 5.8 ± 1.0 in summer (F = 40.235, $p < 0.001$), showing high significance. Progressive enrichment across seasons indicates intensified weathering or carbonate dissolution in warmer periods within the Bartlett pond. *Ca^{2+} (%) value declined inversely from 96.6 ± 0.2 in fall to 95.8 ± 0.1 in spring and 94.2 ± 1.0 in summer (F = 40.235, $p < 0.001$), showing high significance. The inverse trend reflects redistribution of Ca^{2+} from the weathered pool into the sea-salt-contributed fraction, potentially due to resuspension or secondary mineral formation within the pond.

Sulfate (SO_4^{2-}): SS-SO_4^{2-} (%) values varied slightly across seasons (14.3 ± 0.3 in fall, 15.2 ± 0.2 in spring, 14.2 ± 2.6 in summer) with F = 0.959 and $p = 0.004$, indicating statistical significance but with minimal amplitude of variation. The near-constant behavior suggests that sulfate is relatively conservative and less sensitive to seasonal temperature changes, unlike major base cations. *SO_4^{2-} (%) values are similarly stable (85.7 ± 0.3 in fall, 84.8 ± 0.2 in spring, 85.8 ± 2.6 in summer) with F = 0.959 and $p = 0.004$, indicating statistically significant yet minor variability. The concentration of sulfate reflects stable partitioning of sulfate between sea-salt-contributed and weathered fractions, indicating limited influence of temperature on its geochemical cycling. More than 60% of sea-salt-contributed sodium was found in high elevation sites, and more than 80% of sea-salt-contributed sodium to total sodium in low elevation sites was reported in an earlier study from the Rio Icacos watershed in Puerto Rico, while magnesium, sulfate, potassium, and calcium were relatively too low in comparison to the Bartlett pond sites

[45]. In Bartlett pond, average sea-salt-contributed magnesium appeared as 76% of the total magnesium, suggesting marine contribution as the dominant fraction (Figure 2).

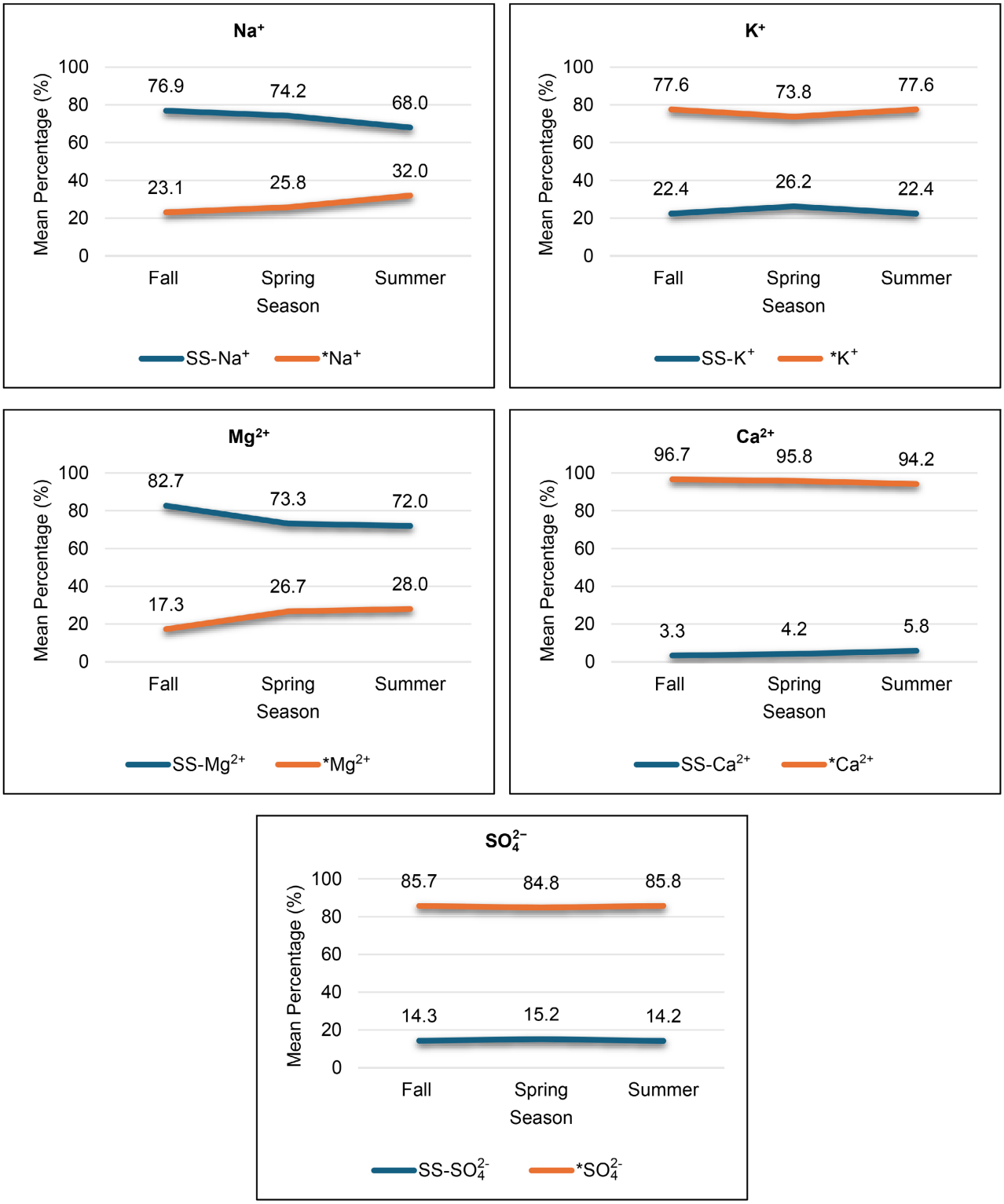

Figure 3. Seasonal variability of sea-salt contribution (SS) and weathered (*) ions within Bartlett Pond.

The ANOVA results collectively demonstrate that temperature-driven seasonal dynamics significantly modulate the ionic balance between sea-salt contributed and weathered pools within Bartlett Pond. Fall seasons are characterized by higher sea-salt contributed fractions (especially Na^+ and Mg^{2+}), likely due to lower dilution and reduced weathering activity or high transfer of marine aerosols due to high-speed wind. Summer seasons show enhanced non-salt (weathered) contributed fractions (notably Na^+, Mg^{2+}, and Ca^{2+}), reflecting intensified weathering, ion exchange, and hydrological flushing. Sulfate remains the least variable, consistent with its conservative ionic nature. These findings underscore the sensitivity of coastal pond geochemistry to seasonal thermal and hydrological shifts, providing valuable insight into the balance between marine aerosol input and terrestrial weathering processes. The composite figure of all five ions (Na^+, K^+, Mg^{2+}, Ca^{2+}, and SO_4^{2-}) is shown in the above **Figure 3**. It clearly illustrates the contrasting seasonal trends between sea-salt contributed (SS) and weathered (*) fractions across ions within Bartlett Pond.

5. Discussion

The regression models presented in **Table 2** encapsulate the interdependence of major ionic species and their collective influence on water quality parameters across seasons within Bartlett Pond. A total of 39 predictive equations were developed for 17 variables, each capturing unique seasonal dynamics. The exceptionally high coefficients of determination ($R^2 = 0.64$ - 1.00) indicate that the selected predictors effectively represent the processes governing the pond's chemical composition. This high explanatory power reflects both the internal chemical coherence of the system and the effectiveness of the chosen statistical approach. Electrical Conductivity (EC) and Total Dissolved Solids (TDS) emerged as key integrative parameters, linking the ionic strength of the solution to multiple biogeochemical processes. Their reciprocal predictive relations highlight the interconnected roles of salinity, ionic mobilization, and nutrient availability within the pond ecosystem.

Across seasons, ionic interrelations reveal a dynamic interplay between evaporative concentration, nutrient cycling, and weathering feedback. During spring, elevated phosphate and sulfate concentrations suggest active biogeochemical cycling following precipitation-mediated recharge. In summer, positive coefficients of boron and nitrate reflect evaporative enrichment and enhanced biological transformation under warmer conditions typical of this hot, semi-arid region of southern Texas. The observed decrease in nitrate in summer is consistent with accelerated photosynthetic activity, where nitrate uptake increases rapidly. Fall models emphasize carbonate regulation and ionic dilution, commonly associated with turnover and rainfall-driven mixing. Cationic predictors such as Ca^{2+} and Mg^{2+} often exhibit negative regression coefficients in warm seasons, suggesting carbonate precipitation or adsorption processes that moderate ionic concentrations within the pond. Conversely, Na^+, Cl^-, and NO_3^- frequently emerge as strong positive contributors, highlighting their solubility and resilience to sea-

sonal geochemical shifts. The suite of regression equations forms an analytical network that quantitatively describes the mutual influence among ions within the pond. This integrated approach reveals that: Nutrient ions (NO_3^-, PO_4^{3-}) act as sensitive tracers of both watershed inputs and internal nutrient cycling. Hale *et al.* (2015) [53] emphasized the complexity of anthropogenic drivers on nutrient (N, P) dynamics and noted that nutrient delivery is linked to human activities within the watershed. Urban runoff and internal biogeochemical processes within the pond therefore shape nutrient concentration. Seasonality increases in temperature, particularly during summer, lead to elevated GPP and correspondingly rapid nitrate uptake, as nitrate utilization scales with productivity. Nitrate uptake varies as a function of GPP in various aquatic ecosystems (e.g., in the macrophyte-dominated Ichetucknee River in Florida, USA, as reported by Bernhardt *et al.* (2018) [54]). SAR and Boron behave as cross-seasonal indicators of ionic exchange and geochemical maturity. The system exhibits tight electrochemical coupling, where variation in one major parameter (e.g., EC or SAR) propagates predictably across multiple solutes. These relationships confirm that Bartlett Pond operates under quasi-equilibrium geochemical control, where natural buffering processes and anthropogenic influence jointly determine solute chemistry. Analysis of variance (ANOVA) revealed that the seasonal variation in Bartlett Pond is both statistically significant and geochemically meaningful. All major ions exhibited distinct patterns between fall, spring, and summer, reflecting the combined effects of hydrological dilution, evaporation, and temperature-mediated chemical weathering.

Sodium (Na^+) showed a strong inverse relationship between sea-salt contributed and weathered fractions. The weathered $*Na^+$ fraction decreased from 76.9% in fall to 68.0% in summer, while $*Na^+$ increased from 23.1% to 32.0% during the same period ($p < 0.001$). This inverse trend indicates that higher summer temperatures enhance desorption and cation exchange processes, transferring Na^+ from the sea-salt pool to the weathered phase. **Potassium (K^+)** displayed a moderate but statistically significant variation ($p < 0.001$). Sea-salt contributed ($SS\text{-}K^+$) peaked in spring (26.2%) compared to fall and summer (~22%), while weathered $*K^+$ exhibited the reverse pattern. This springtime peak may reflect enhanced biogeochemical cycling or the leaching of particulate matter following seasonal precipitation, prior to dilution or biological uptake in summer. **Magnesium (Mg^{2+})** followed a similar pattern to sodium. The sea-salt Mg^{2+} ($SS\text{-}Mg^{2+}$) decreased from 82.7% in fall to 72.0% in summer, while weathered ($*Mg^{2+}$) increased from 17.3% to 28.0% ($p = 0.004$). The shift indicates temperature-enhanced mineral dissolution and ionic mobilization, consistent with intensified weathering and cation exchange during summer. **Calcium (Ca^{2+})** exhibited the most pronounced seasonal variation. The sea-salt contributed ($SS\text{-}Ca^{2+}$) fraction rose sharply from 3.4% in fall to 5.8% in summer, while the weathered contributed ($*Ca^{2+}$) fraction declined from 96.6% to 94.2% ($p < 0.001$). These changes suggest that warmer temperatures promote carbonate dissolution and increase Ca^{2+} availability in the water column within the pond. Calcium's strong variability makes it a sensitive tracer of geo-

chemical equilibrium between pond water and sedimentary carbonates. **Sulfate (SO_4^{2-})**, while statistically significant ($p = 0.004$), displayed the least seasonal variation, with sea-salt contributions (SS-SO_4^{2-}) remaining between 14% - 15%, and weathered fractions (*SO_4^{2-}) near 85%, indicating sulfate's relatively conservative behavior. This suggests that sulfate's distribution is less temperature-dependent, possibly dominated by stable redox conditions or low biological uptake.

Collectively, these patterns demonstrate that Bartlett Pond experiences dynamic seasonal exchanges between sea-salt and weathered ionic fractions driven by seasonal hydrological and thermal gradients. Fall conditions favor high sea-salt contributions due to reduced runoff, elevated evaporation, and concentration effects. As temperature rises, ionic re-equilibration favors the release of cations (Na^+, K^+, Mg^{2+}, Ca^{2+}) into the weathered phase due to intensified chemical weathering, leaching, and biological turnover. The consistent inverse relationships between sea-salt and non-sea-salt fractions indicate that the pond maintains a quasi-equilibrium between marine input and terrestrial weathering. Differences in seasonal responsiveness among ions reflect element-specific control, including source strength (Ca^{2+}, Mg^{2+}), and desorption dynamics for (Na^+ and K^+).

These findings align with the broader understanding that small ponds in close proximity to the coast within a hot semi-arid landscape function as biogeochemical sentinels, where temperature and hydrology rapidly influence ion exchange, mineral dissolution, and nutrient availability. Williamson *et al.* (2008) [55] previously emphasized the role of inland waters as sentinels of environmental change and integrators of human impacts. The clear seasonal pattern observed here provides quantitative evidence of climate-weathering coupling in semi-arid environments such as Laredo, Texas.

The scatter plot (**Figure 4**) shows the relationship between sulfate (SO_4^{2-}) and bicarbonate (HCO_3^-) concentrations in Bartlett Pond water samples. The data points reveal a negative correlation, as indicated by the regression line with the equation $SO_4^{2-} = -0.33HCO_3^- + 161.72$ and an R^2 value of 0.38, suggesting a moderate inverse relationship: higher bicarbonate concentrations correspond to lower sulfate concentrations (**Figure 4**).

This trend may indicate geochemical processes such as carbonate buffering and sulfate reduction. In natural waters, higher bicarbonate often reflects increased carbonate weathering or buffering capacity, which can occur in less acidic conditions. Conversely, elevated sulfate levels are commonly associated with oxidation of sulfide minerals or anthropogenic inputs. The inverse relationship suggests that as bicarbonate increases, possibly due to carbonate dissolution or neutralization, sulfate concentrations decrease, which could be linked to dilution effects or microbial sulfate reduction under more alkaline conditions. Based on our observation, pond water is alkaline (**Table 2**), and hence microbial sulfate reduction is the most probable explanation for the decrease in sulfate with an increase in bicarbonate. This pattern provides insight into the pond's chemical balance and potential influences from underlying lithology or biological activity.

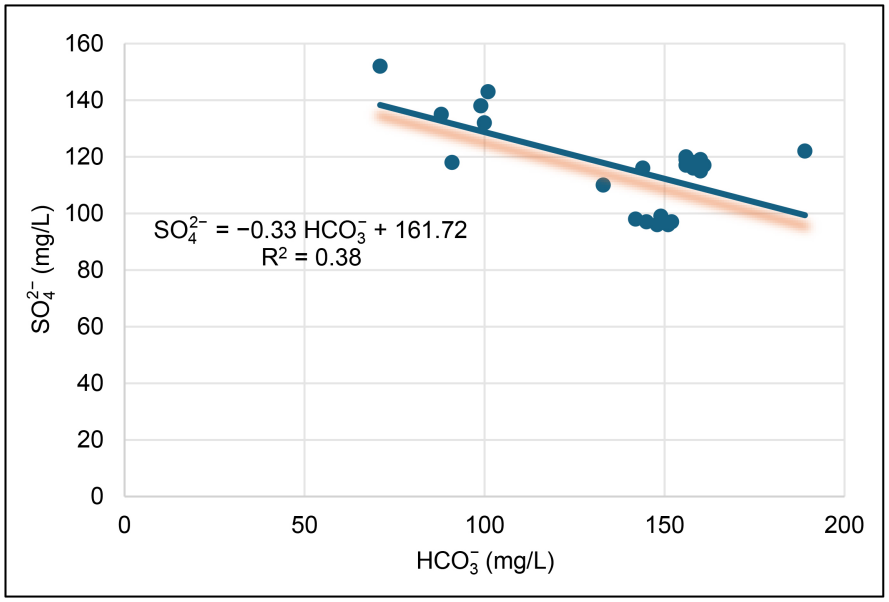

Figure 4. Relationship between sulfate (SO_4^{2-}) and bicarbonate (HCO_3^-) concentrations in Bartlett Pond.

6. Conclusion

Water samples from Bartlett Pond, a small shallow urban wetland in Laredo, southern Texas, were analyzed to evaluate the factors controlling water quality parameters and their spatiotemporal trends. The major cations and anions occurred in the order $Na^+ \gg Ca^{2+} > Mg^{2+} \approx K^+$ and $HCO_3^- \approx Cl^- > SO_4^{2-} \gg NO_3^- \gg PO_4^{3-}$, respectively. Distinct spatial patterns were not observed overall; however, localized variations in nutrient concentrations were evident at sites with dense vegetation and at points receiving direct urban runoff. Natural chemical weathering contributed to the solute load, but marine aerosols (sea-salt inputs) accounted for approximately 76% of total magnesium and 73% of total sodium concentrations. In contrast, calcium, sulfate, and potassium showed higher contributions from chemical weathering processes. Calcite and siliciclastic weathering therefore appear to be the dominant geochemical controls after sea-salt inputs. Nitrate concentrations decreased sharply during summer compared with fall and spring, suggesting enhanced photosynthetic activity and increased gross primary productivity (GPP), with phosphate acting as a limiting nutrient. Evidence of sulfate reduction indicates microbial activity under alkaline pond conditions. Anthropogenic inputs, particularly urban runoff, and dry atmospheric deposition also contribute measurable chemical loads to the system. Despite the acceptable limits of sodium adsorption ratios (SAR < 4), the overall water quality is not suitable for most uses, including irrigation, because of existing trace metals contamination that we reported earlier.

Study Limitations

Temporal limitation: Data represent only three discrete seasonal snapshots (fall,

spring, summer) within one annual cycle, limiting the long-term interpretation of interannual variability. **Spatial limitation:** Sampling was confined to a single pond; site-specific hydrological and geochemical characteristics may not represent broader coastal systems. **Analytical limitation:** The dataset focuses on major ions only; exclusion of dissolved organic matter, dissolved silica, all forms of dissolved inorganic carbon, and minor or trace elements may underestimate the full biogeochemical response to seasonal forcing.

Future Research Directions

Future work could integrate continuous year-round sampling with expanded chemical and isotopic measurements to evaluate the temporal stability of observed trends. Combining these results with hydrological modeling and climate projections would enable a predictive framework linking temperature fluctuations to ionic cycling and weathering intensity. Additionally, comparative analyses across multiple coastal ponds could elucidate whether Bartlett Pond's behavior typifies regional-scale sea salt contribution and chemical weathering dynamics under changing climatic regimes.

Acknowledgements

The authors would like to thank Aaron Perez at the Center for Earth and Environmental Studies of Texas A & M International University for his help in producing the sampling area map (Figure 1). The authors acknowledge the Welch Foundation Grant No. BS-0051 for supporting this research. Authors would like to thank the editorial office for their proficient handling of the manuscript. Authors are also grateful to the editors and anonymous reviewers for their valuable suggestions and insightful comments, which have significantly strengthened the paper.

Authors' Contributions

MPB designed and implemented the project, conducted the chemistry data analysis, and led the manuscript writing, reviewing, and editing; DEN carried out field sampling and contributed to writing and reviewing; SB assisted with chemistry data processing and contributed to writing and reviewing. GBM performed data analysis using multivariate modeling and contributed to writing, reviewing, and editing. AAM contributed to methodology development, funding acquisition, writing, reviewing, and editing.

Conflicts of Interest

The authors declare no conflicts of interest regarding the publication of this paper.

References

[1] Bayart, J., Bulle, C., Deschênes, L., Margni, M., Pfister, S., Vince, F., *et al.* (2010) A Framework for Assessing Off-Stream Freshwater Use in LCA. *The International*

Journal of Life Cycle Assessment, **15**, 439-453. https://doi.org/10.1007/s11367-010-0172-7

[2] Vörösmarty, C.J., McIntyre, P.B., Gessner, M.O., Dudgeon, D., Prusevich, A., Green, P., *et al.* (2010) Global Threats to Human Water Security and River Biodiversity. *Nature*, **467**, 555-561. https://doi.org/10.1038/nature09440

[3] Pradinaud, C., Northey, S., Amor, B., Bare, J., Benini, L., Berger, M., *et al.* (2019) Defining Freshwater as a Natural Resource: A Framework Linking Water Use to the Area of Protection Natural Resources. *The International Journal of Life Cycle Assessment*, **24**, 960-974. https://doi.org/10.1007/s11367-018-1543-8

[4] Bhatt, M.P., Malla, G.B. and McDowell, W.H. (2024a) Comprehensive Assessment and Analysis of Drinking Water Quality in the Kathmandu Valley: Implications for Public Health and Policy. *American Journal of Water Resources*, **12**, 149-164. https://doi.org/10.12691/ajwr-12-4-5

[5] Wang, Y. (2025) Spatial-Temporal Variation and Risk Assessment of Water Quality. *Water*, **17**, Article 2872. https://doi.org/10.3390/w17192872

[6] Vörösmarty, C.J., Green, P., Salisbury, J. and Lammers, R.B. (2000) Global Water Resources: Vulnerability from Climate Change and Population Growth. *Science*, **289**, 284-288. https://doi.org/10.1126/science.289.5477.284

[7] UNEP (2002) The Global Environment Outlook 3, Past, Present and Future Perspectives. Earthscan Publications Ltd., 466.

[8] MacDonald, G.M. (2010) Water, Climate Change, and Sustainability in the Southwest. *Proceedings of the National Academy of Sciences*, **107**, 21256-21262. https://doi.org/10.1073/pnas.0909651107

[9] Pekel, J., Cottam, A., Gorelick, N. and Belward, A.S. (2016) High-Resolution Mapping of Global Surface Water and Its Long-Term Changes. *Nature*, **540**, 418-422. https://doi.org/10.1038/nature20584

[10] Tickner, D., Opperman, J.J., Abell, R., Acreman, M., Arthington, A.H., Bunn, S.E., *et al.* (2020) Bending the Curve of Global Freshwater Biodiversity Loss: An Emergency Recovery Plan. *BioScience*, **70**, 330-342. https://doi.org/10.1093/biosci/biaa002

[11] Ostad-Ali-Askari, K. (2022) Review of the Effects of the Anthropogenic on the Wetland Environment. *Applied Water Science*, **12**, Article No. 260. https://doi.org/10.1007/s13201-022-01767-4

[12] Bhatt, M.P., Rubio, A., Malla, G.B., Lopez, C., Morales, V., Cano, E.V., *et al.* (2024b) Evaluation of Human Impacts on Bartlett Pond Ecosystem, Laredo, Southern Texas, USA, through Empirical Modeling. *Journal of Environmental Protection*, **15**, 497-526. https://doi.org/10.4236/jep.2024.154029

[13] Bhatt, M.P., Malla, G.B., Rubio, A. and Addo-Mensah, A. (2025a) Sediment Quality Assessment on Bartlett Pond in Laredo, Southern Texas, Usa. *Open Journal of Soil Science*, **15**, 43-69. https://doi.org/10.4236/ojss.2025.151003

[14] Gavrilaş, S., Burescu, F., Chereji, B. and Munteanu, F. (2025) The Impact of Anthropogenic Activities on the Catchment's Water Quality Parameters. *Water*, **17**, Article 1791. https://doi.org/10.3390/w17121791

[15] Greenwood, E.E., Lauber, T., van den Hoogen, J., Donmez, A., Bain, R.E.S., Johnston, R., *et al.* (2024) Mapping Safe Drinking Water Use in Low- and Middle-Income Countries. *Science*, **385**, 784-790. https://doi.org/10.1126/science.adh9578

[16] Hope, R. (2024) Four Billion People Lack Safe Water. *Science*, **385**, 708-709. https://doi.org/10.1126/science.adr3271

[17] Soliman, A. (2024) 'Unacceptable': A Staggering 4.4 Billion People Lack Safe Drink-

ing Water, Study Finds. *Nature*, **632**, 964-965.
https://doi.org/10.1038/d41586-024-02621-0

[18] Kundu, S., Kundu, B., Rana, N.K. and Mahato, S. (2024) Wetland Degradation and Its Impacts on Livelihoods and Sustainable Development Goals: An Overview. *Sustainable Production and Consumption*, **48**, 419-434.
https://doi.org/10.1016/j.spc.2024.05.024

[19] Ramsar (2006) The Ramsar Convention Manual: A Guide to Convention on Wetlands. 4th Edition, The Ramsar Convention Secretariat, 114 p.

[20] Meli, P., Rey Benayas, J.M., Balvanera, P. and Martínez Ramos, M. (2014) Restoration Enhances Wetland Biodiversity and Ecosystem Service Supply, but Results Are Context-Dependent: A Meta-Analysis. *PLOS ONE*, **9**, e93507.
https://doi.org/10.1371/journal.pone.0093507

[21] Turner, K. (1991) Economics and Wetland Management. *Ambio*, 20, 59-63.

[22] Mitsch, W.J. and Gosselink, J.G. (1993) Wetlands. Second Edition. Van Nostrand Reinhold.

[23] Mitsch, W.J. and Gosselink, J.G. (2000) The Value of Wetlands: Importance of Scale and Landscape Setting. *Ecological Economics*, **35**, 25-33.
https://doi.org/10.1016/s0921-8009(00)00165-8

[24] Bhatt, M.P., Bhatt, S. and Gaye, B. (2013) Controls on Pond Water Chemistry within Kathmandu Valley, Nepal. *International Journal of Lakes and Rivers*, **6**, 153-172.

[25] Tokatli, C. (2017) Bioecological and Statistical Risk Assessment of Toxic Metals in Sediments of a Worldwide Important Wetland: Gala Lake National Park (Turkey). *Archives of Environmental Protection*, **43**, 34-47.
https://doi.org/10.1515/aep-2017-0007

[26] Cunningham, W. and Cunningham, M. (2021) Environmental Science: A Global Concern. The McGraw Hill Companies Inc., 15th Edition, 375 p.

[27] Hill, M.J., Greaves, H.M., Sayer, C.D., Hassall, C., Milin, M., Milner, V.S., *et al.* (2021) Pond Ecology and Conservation: Research Priorities and Knowledge Gaps. *Ecosphere*, **12**, e03853. https://doi.org/10.1002/ecs2.3853

[28] Keddy, P.A. (2023) Wetland Ecology. 3rd Edition, Cambridge University Press, 566.
https://doi.org/10.1017/9781009288675

[29] Conservation on Wetlands (2025) Global Wetland Outlook 2025: Valuing, Conserving, Restoring and Financing Wetlands. Gland, Switzerland, Secretariat of the Convention on Wetlands, 80 p.

[30] Reis, V., Hermoso, V., Hamilton, S.K., Ward, D., Fluet-Chouinard, E., Lehner, B., *et al.* (2017) A Global Assessment of Inland Wetland Conservation Status. *BioScience*, **67**, 523-533. https://doi.org/10.1093/biosci/bix045

[31] Osbourne, P.L. and Adcock, P.W. (1995) Creating Environmental Kidneys: Wetlands Ecosystems as Pollution Filters and Habitat Restoratives. *Wetlands Australia*, **14**, 37-43. https://doi.org/10.31646/wa.176

[32] Sharifi, A., Kalin, L., Hantush, H., and Isik, S. (2013) Wetlands: Earth's Kidneys. In: Lamar, J. and Lockaby, B.G., Eds., *Auburn Speaks*, Auburn University, 140-143.

[33] Downing, J.A., Prairie, Y.T., Cole, J.J., Duarte, C.M., Tranvik, L.J., Striegl, R.G., *et al.* (2006) The Global Abundance and Size Distribution of Lakes, Ponds, and Impoundments. *Limnology and Oceanography*, **51**, 2388-2397.
https://doi.org/10.4319/lo.2006.51.5.2388

[34] Céréghino, R., Boix, D., Cauchie, H., Martens, K. and Oertli, B. (2014) The Ecological

Role of Ponds in a Changing World. *Hydrobiologia*, **723**, 1-6. https://doi.org/10.1007/s10750-013-1719-y

[35] Zou, Z., Huang, C., Lang, M.W., Du, L., McCarty, G., Ingebritsen, J.C., *et al.* (2024) Hotspots of Wetland Loss to Impervious Surfaces in the Conterminous United States. *Science of The Total Environment*, **948**, Article 174787. https://doi.org/10.1016/j.scitotenv.2024.174787

[36] Rosen, R.A. (2015) Texas Aquatic Science. Texas A&M University Press, 234.

[37] ABA (2022) Tenth Annual Laredo Birding Festival. Celebrating Ten Years of Birding the Border. American Birding Association.

[38] Zhang, X., Zhong, Z., Zhang, M., Zhao, F., Wu, Y., Sun, Y., *et al.* (2025) Analysis of Anthropogenic Disturbance and Spatial and Temporal Changes of Bird Communities in Plateau Wetlands Fusing Bird Survey and Nighttime Light Remote Sensing Data. *Journal of Environmental Management*, **375**, Article 124349. https://doi.org/10.1016/j.jenvman.2025.124349

[39] Pandey, J. and Singh, R. (2017) Heavy Metals in Sediments of Ganga River: Up- and Downstream Urban Influences. *Applied Water Science*, **7**, 1669-1678. https://doi.org/10.1007/s13201-015-0334-7

[40] Baran, A., Tarnawski, M., Koniarz, T. and Szara, M. (2019) Content of Nutrients, Trace Elements, and Ecotoxicity of Sediment Cores from Rożnów Reservoir (Southern Poland). *Environmental Geochemistry and Health*, **41**, 2929-2948. https://doi.org/10.1007/s10653-019-00363-x

[41] Klink, A., Dambiec, M. and Polechońska, L. (2019) Trace Metal Speciation in Sediments and Bioaccumulation in Phragmites Australis as Tools in Environmental Pollution Monitoring. *International Journal of Environmental Science and Technology*, **16**, 7611-7622. https://doi.org/10.1007/s13762-019-02305-7

[42] Bhatt, M.P., Malla, G.B. and Yde, J.C. (2025b) Status and Progress of Determining the Variability and Controls on Chemical Denudation Rates in Glacierized Basins around the World. *Water*, **17**, Article 2811. https://doi.org/10.3390/w17192811

[43] McDowell, W.H., Sánchez, C.G., Asbury, C.E. and Ramos Pérez, C.R. (1990) Influence of Sea Salt Aerosols and Long Range Transport on Precipitation Chemistry at El Verde, Puerto Rico. *Atmospheric Environment. Part A. General Topics*, **24**, 2813-2821. https://doi.org/10.1016/0960-1686(90)90168-m

[44] Millot, R., Gaillardet, J., Dupré, B. and Allègre, C.J. (2002) The Global Control of Silicate Weathering Rates and the Coupling with Physical Erosion: New Insights from Rivers of the Canadian Shield. *Earth and Planetary Science Letters*, **196**, 83-98. https://doi.org/10.1016/s0012-821x(01)00599-4

[45] Bhatt, M.P. and McDowell, W.H. (2007) Controls on Major Solutes within the Drainage Network of a Rapidly Weathering Tropical Watershed. *Water Resources Research*, **43**, W11402. https://doi.org/10.1029/2007wr005915

[46] US Climate (2025) Climate Data of Laredo. https://www.usclimatedata.com/climate/laredo/texas/united-states/utstx0737

[47] US EPA (1991) Methods for Determination of Metals in Environmental Samples. EPA/600/4-91/010, Office of Research and Development.

[48] APHA (1989) Standard Methods for the Examination of Water and Wastewater. American Public Health Association.

[49] Bhatt, M.P., Takeuchi, N. and Acevedo, M.F. (2016) Chemistry of Supraglacial Ponds in the Debris-Covered Area of Lirung Glacier in Central Nepal Himalayas. *Aquatic Geochemistry*, **22**, 35-64. https://doi.org/10.1007/s10498-015-9276-9

[50] Bhatt, M.P., Hartmann, J. and Acevedo, M.F. (2018) Seasonal Variations of Biogeochemical Matter Export along the Langtang-Narayani River System in Central Himalaya. *Geochimica et Cosmochimica Acta*, **238**, 208-234. https://doi.org/10.1016/j.gca.2018.06.033

[51] Tartari, G., Tartari, G. and Mosello, R. (1998) Water Chemistry of High Altitude Lakes in the Khumbhu and Imja Khola Valley, (Nepalese Himalaya). Limnology of High Altitude Lakes in the Mt. Everest Region (Nepal). *Journal of Limnology*, **57**, 51-76.

[52] Bhatt, M.P. and Malla, G.B. (2025) Spatiotemporal Variations of Inorganic Carbon Species along the Langtang-Narayani River System, Central Himalaya. *Water*, **17**, Article 2727. https://doi.org/10.3390/w17182727

[53] Hale, R.L., Grimm, N.B., Vörösmarty, C.J. and Fekete, B. (2015) Nitrogen and Phosphorus Fluxes from Watersheds of the Northeast U.S. from 1930 to 2000: Role of Anthropogenic Nutrient Inputs, Infrastructure, and Runoff. *Global Biogeochemical Cycles*, **29**, 341-356. https://doi.org/10.1002/2014gb004909

[54] Bernhardt, E.S., Heffernan, J.B., Grimm, N.B., Stanley, E.H., Harvey, J.W., Arroita, M., *et al.* (2018) The Metabolic Regimes of Flowing Waters. *Limnology and Oceanography*, **63**, S99-S118. https://doi.org/10.1002/lno.10726

[55] Williamson, C.E., Dodds, W., Kratz, T.K. and Palmer, M.A. (2008) Lakes and Streams as Sentinels of Environmental Change in Terrestrial and Atmospheric Processes. *Frontiers in Ecology and the Environment*, **6**, 247-254. https://doi.org/10.1890/070140